

STRUCTURE OF A NEW ORTHORHOMBIC PHASE IN TiNi-Mn SHAPE MEMORY ALLOYS

Lajos Tóth[†], Jenő Beyer

University of Twente, Fac. Mechanical Engineering, POB 217, 7500 AE Enschede, The Netherlands
[†] on leave from Research Institute for Technical Physics, Budapest, Hungary

(Received November 27, 1990)

Introduction

The thermoelastic martensitic transformation causing the shape memory effect in nearly equi-atomic TiNi alloys has long been studied [1]. The crystallographic structure of both the monoclinic martensite phase and the rhombohedral premartensitic phase (known as R-phase) as well as their orientation relationship to the ordered bcc austenite (parent phase) has been determined [2]. Beside the stable intermetallic phases (Ti₂Ni, TiNi, TiNi₃) several metastable phases with various crystallographic structures (rhombohedral, hexagonal, monoclinic, cubic) have also been reported to precipitate due to suitable annealing treatments [3, 4].

The microstructural changes taking place in TiNi alloys during their reversible martensitic transformation can best be studied by transmission electron microscopy (TEM) at around room temperature. Since the characteristic temperatures of the martensitic transformation are rather sensitive to any change of the stoichiometry, a slight change of Ni to Ti ratio or the addition of some ternary element might result in a shift of transformation temperature to a value below room temperature. In contrast to earlier work of Honma et al [5] it has been verified that Mn added to TiNi lowers the transformation temperature rather strongly [6]. This enables us to make a detailed TEM observation of the defect structure of the samples in the austenite state at room temperature. In the present paper a new intermetallic phase is described which has been observed in NiTi-Mn samples during the TEM study of the martensitic transformation process. Preliminary results of the study have been published [7].

Experimental

TiNi-Mn samples have been prepared by arc melting pieces of Ti (99.98 % purity), Ni (99.9985 %) and Mn (99.95 %). The samples were repeatedly remelted in argon atmosphere and homogenized at 950 °C for 72 hours in high vacuum in an infrared furnace followed by furnace cooling. A part of the ingots was then subjected to hot deformation of 10% at 800 °C. After spark cutting slices of 0.2 mm thickness, TEM specimens were prepared from both annealed and deformed samples by electrochemical polishing with the twin-jet technique in methanol-perchloric acid electrolyte kept at -10 to -30 °C. The TEM study was carried out in a JEOL 200 CX analytical electron microscope operating at 200 kV. The composition of the samples as determined by electron probe microanalysis (EDS) is presented in Table 1.

Results

The differential scanning calorimetry (DSC) measurements revealed that the addition of Mn shifted the Ms temperature of TiNi to lower values with a rate of about 60 °C/at% Mn (Table 1) [6]. However it did not influence so much the formation temperature of R-phase on cooling which caused therefore the separation of the R-phase formation from that of the martensite resulting in two peaks in the DSC curves (Fig. 1).

The room temperature crystal structure of the annealed samples of TiNi-Mn has been found by TEM to change with Mn content from martensite (with no Mn addition) through a mixture of martensite and austenite to pure austenite (samples with higher than 1% Mn). The presence of the martensite

in the TEM-samples with 0.9 at% Mn at room temperature might be the consequence of the electro polishing being made at temperatures of less than -10°C . Equiaxed Ti_3Ni precipitates caused by the excess amount of Ti have also been observed in all samples distributed along the grain boundaries of the matrix.

TABLE 1

EDS Composition (at%) and Transformation Temperature ($^{\circ}\text{C}$) of the Samples in Annealed State

| Sample | Ti | Ni | Mn | Ms |
|--------|-------|-------|--------|--------------------------|
| 01 | 50.56 | 49.43 | (0.01) | 53 $^{\circ}\text{C}$ |
| 15 | 50.61 | 48.49 | 0.90 | -7 $^{\circ}\text{C}$ |
| 02 | 49.95 | 48.71 | 1.34 | -35 $^{\circ}\text{C}$ |
| 04 | 48.44 | 47.01 | 4.54 | <-125 $^{\circ}\text{C}$ |

During the TEM study of the martensitic transformation a new intermetallic phase was observed in the annealed samples with 0.9 and 1.3 at% Mn. This new phase coexisted with either martensite or the austenite phases (Fig. 2) depending on the actual thermal history of the sample. Despite its inhomogeneous distribution this phase is found rather easily by TEM due to the relatively large size of its clusters (in the order of $1\ \mu\text{m}$); however its volume ratio is too small to be observed by X-ray diffraction. The amount of the new phase was somewhat larger in the sample with 0.9 at% Mn where it has been found not only in annealed but also in hot deformed state.

The morphology of this phase showing a lamellar substructure closely resembles that of the martensite phase; however it does not show any structural transformation between -196 and $+100^{\circ}\text{C}$. Contrary to this the austenite phase coexisting with the new phase at room temperature transformed to martensite at about 0 to -35°C during the in situ cooling experiments. Preliminary EDS analysis carried out on the thinned specimens did not show any observable deviation of the composition of the new phase from that of the matrix. The Mn-content does not seem to play a role in the formation of the new phase since the same diffraction pattern had earlier been reported in binary TiNi , then interpreted as "massive martensite" [8].

Electron diffraction patterns of the new phase taken at several orientation of the samples (Fig. 3) allowed us to determine the crystal structure to be orthorhombic with the lattice parameters:

$$a_0 = 0.898\ \text{nm} \quad b_0 = 0.763\ \text{nm} \quad c_0 = 0.483\ \text{nm}$$

The orientation relationship of the new orthorhombic phase to the cubic austenite phase is fixed:

$$(001)_0 \parallel (111)_c \quad \text{and} \quad [100]_0 \parallel [110]_c$$

This orientation relationship allows for the formation of three variants of the orthorhombic phase for each of the possible four $\langle 111 \rangle$ zone axes, the largest axis of their elementary cell lying along one of the three $\langle 110 \rangle_c$ directions of the $[111]_c$ zone. Those variants belonging to the same $[111]_c$ zone have a twin-related orientation. This configuration has often been observed experimentally resulting in spectacular composite diffraction patterns of threefold symmetry (Fig. 4). The principal crystallographic axes of the O-phase coincide with low index directions in the cubic lattice:

$$[100]_0 = 2x[110]_c, \quad [010]_0 = [112]_c, \quad [001]_0 = [111]_c$$

The elementary cell of the new orthorhombic phase can thus be constructed from 12 elementary cells of the cubic phase by introducing a 7.5% compression in the $[111]_c$ direction and a 5.3% and 3.3% expansion in the $[110]_c$ and $[112]_c$ directions respectively. The resulting increase of the elementary cell volume is 0.4%. This compares well with the volume change of the lattice (0.3 - 0.4%) during the austenite - martensite transformation. At this moment it is not clear whether this compression in the $[111]_c$ direction is of the same type as in the case of the R-phase formation which is common in these alloys (Fig. 1).

Streaks in the $[100]_0$ directions of the ED patterns indicate the presence of stacking faults in most grains of the O-phase (Fig. 4 and 5). Measurements on the $[001]_0$ zone lattice images (Fig. 5) suggest a local variation of the stacking sequence of $(100)_0$ atomic layers originating from $(110)_c$ layers. Apart of the stacking faults other defects (B in Fig.6) have also been observed which are interpreted as antiphase boundaries (APB) with a displacement vector parallel to the electron beam. Since the latter direction ($[001]_0$ or $[111]_c$) is the same as the direction of the Burgers vector for APB in the ordered bcc lattice ($1/2 \langle 111 \rangle_c$) we assume that these defects in the O-phase have been inherited from the ordered bcc austenite phase. The presence of this type of APBs in the austenite phase has been confirmed in our samples.

In situ heat treatment of the samples in the electron microscope caused the new phase to transform into the austenite phase above about 200 °C (Fig. 7). The higher decomposition temperature may be the result of the larger volume change during the transformation as compared to the martensite. Contrary to the martensite, however, its decomposition seems to be irreversible since it did not appear again after several weeks ageing at room temperature neither as a result of dipping into liquid nitrogen for some minutes. Beside the cubic austenite reflections, instead, faint superstructure reflections could be observed by electron diffraction after the ageing at 1/2 and 1/4 distances of the principal spots. This kind of diffraction pattern has been reported by [8, 9] and classified as "thin film artifact" [9] connected to surface oxidation of the thinned sample which cannot be excluded in the applied experimental conditions.

Conclusion

The results of the TEM study together with the heating experiments led us to the conclusion that the observed new orthorhombic phase is a metastable transformation product. Although no direct relation seems to exist to the martensitic transformation it is suggested that the formation of the orthorhombic phase must be preceded by a cooling down to or below the martensitic transformation temperature. The mechanism of its formation seems to be closely related to that of the R-phase.

Acknowledgements

The authors are deeply indebted to Yin Jian for the preparation of the samples and performing the DSC measurements.

References

1. G.R. Purdy and J.G. Parr, Met. Trans. 221, 636 (1961)
2. K. Otsuka, T. Sawamura and K. Shimizu, Phys. Stat. Sol. (a) 5, 457 (1971)
3. J. Beyer, R.A. v.d.Brakel and J.R.T. Lloyd, Proc. Int. Conf. Martensitic Transformation, P. 703, Japan Inst. Metals, (1986)
4. M. Nishida and C. M. Wayman, Mater. Sci. Eng. 93, 191 (1987)
5. T. Honma, M. Matsumoto, Y. Shugo, M. Nishida and Y. Yamazaki, Proc. 4th Int. Conf. on Titanium (ed. H. Kimura and O. Izumi), p. 1455 (1980)
6. P.M. Huisman-Kleinherenbrink, Yin Jian and J. Beyer, to be published in Materials Letters
7. J. Beyer and L. Tóth, Proc. XII. Int. Congress on Electron Microscopy, Vol. 4, p. 1000, San Francisco Press Inc. (1990)
8. S. R. Zijlstra, J. Beyer and J.A. Klostermann, J. Mater. Sci. 9, 145 (1974)
9. P. Moine, E. Goo and R. Sinclair, Scripta Metall. 18, 1143 (1984)

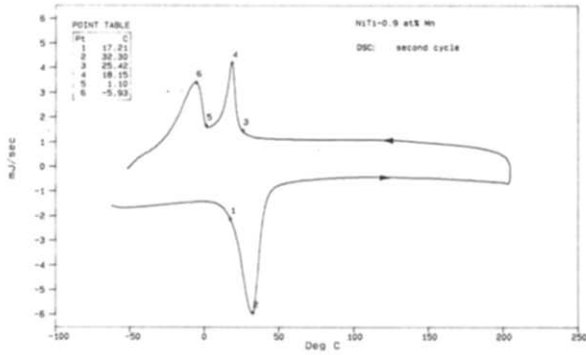


FIG. 1. DSC curve of NiTi-0.9 at% Mn sample (2nd cycle).

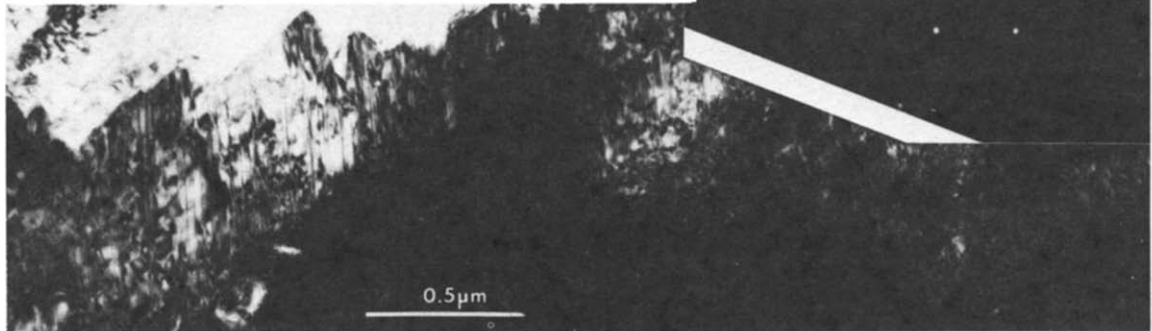


FIG. 2. TEM micrograph and SAD pattern of the new phase in NiTi-Mn surrounded by martensite.

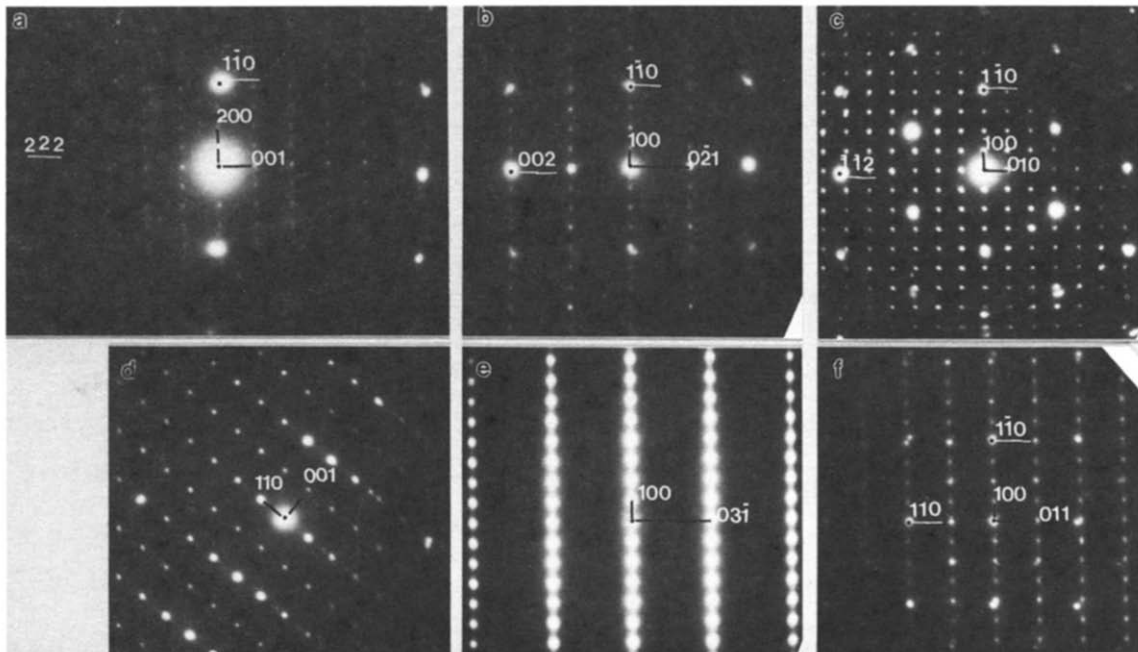


FIG. 3. Selected area diffraction patterns of the orthorhombic phase at various orientations: (a) [010] zone, (b) [012] zone, (c) [001] zone, (d) [110] zone, (e) [013] zone and (f) [011] zone.

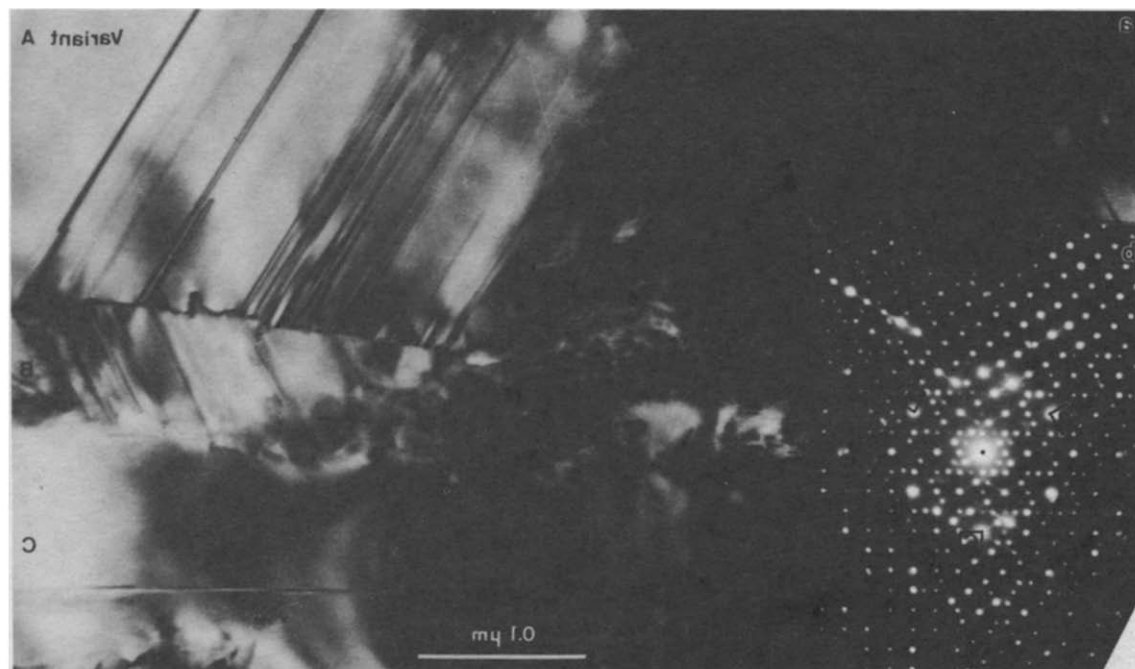


FIG. 4. Bright field image (a) of three variants and their composite SAD pattern (b). Variants A and B are faulted. From Proc. XII. ICEM, @ San Francisco Press Inc., by permission.

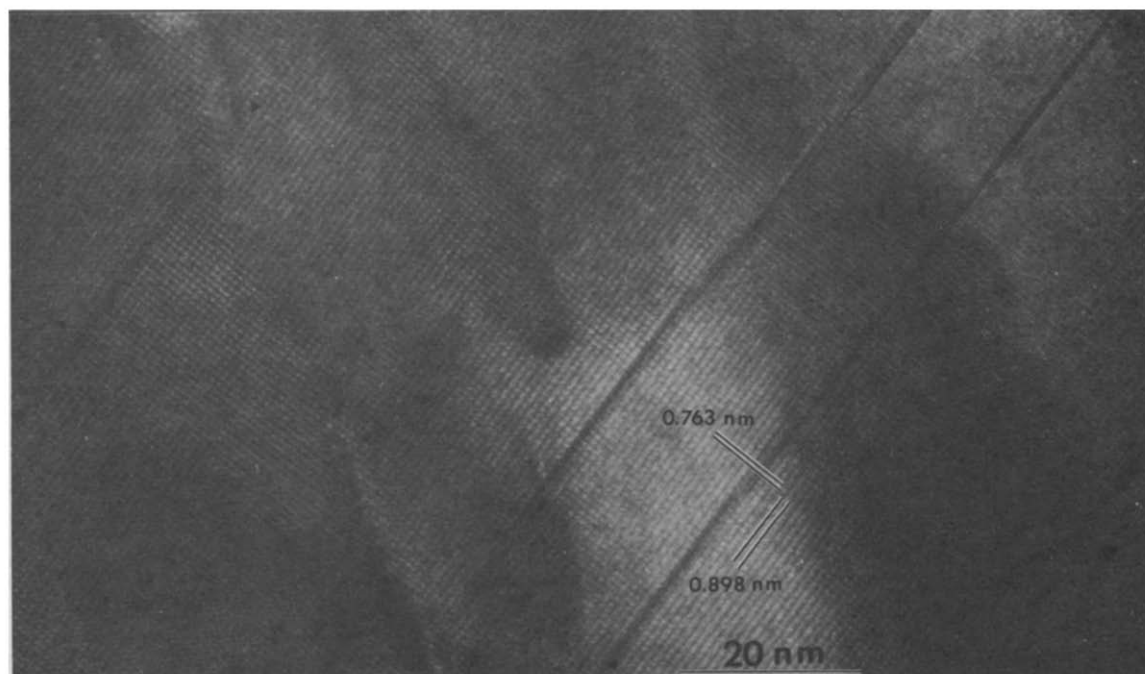


FIG. 5. [001] zone lattice image of the orthorhombic phase with planar defects (stacking faults) along the (100) planes.

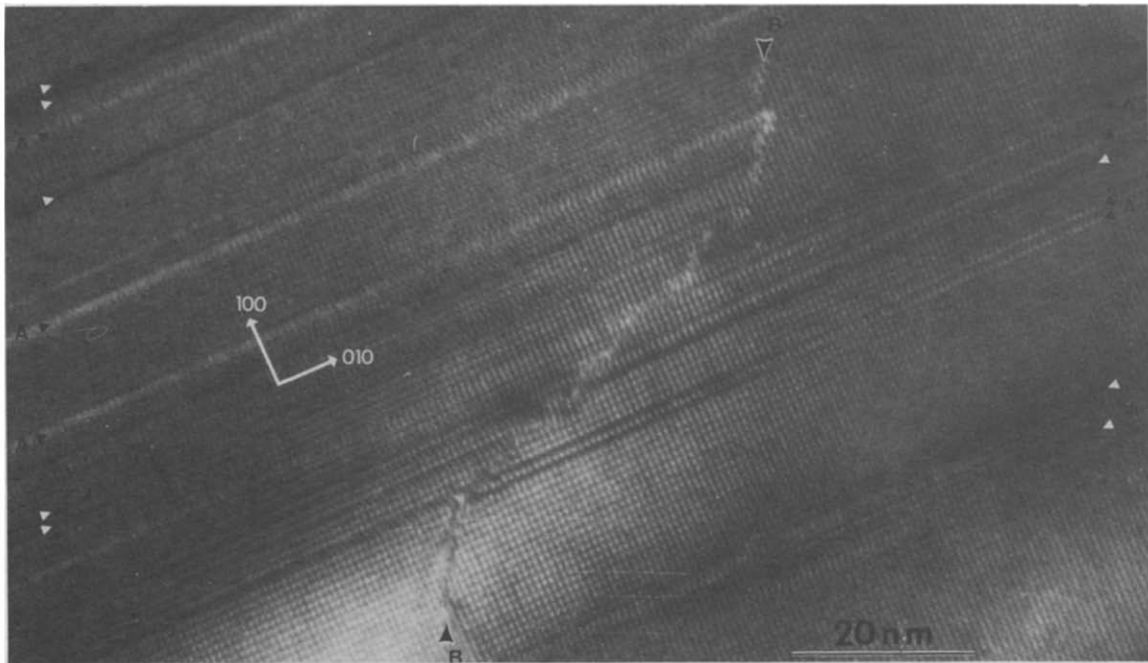


FIG. 6. [001] zone lattice image of the new phase with (A) stacking faults and (B) antiphase boundary.

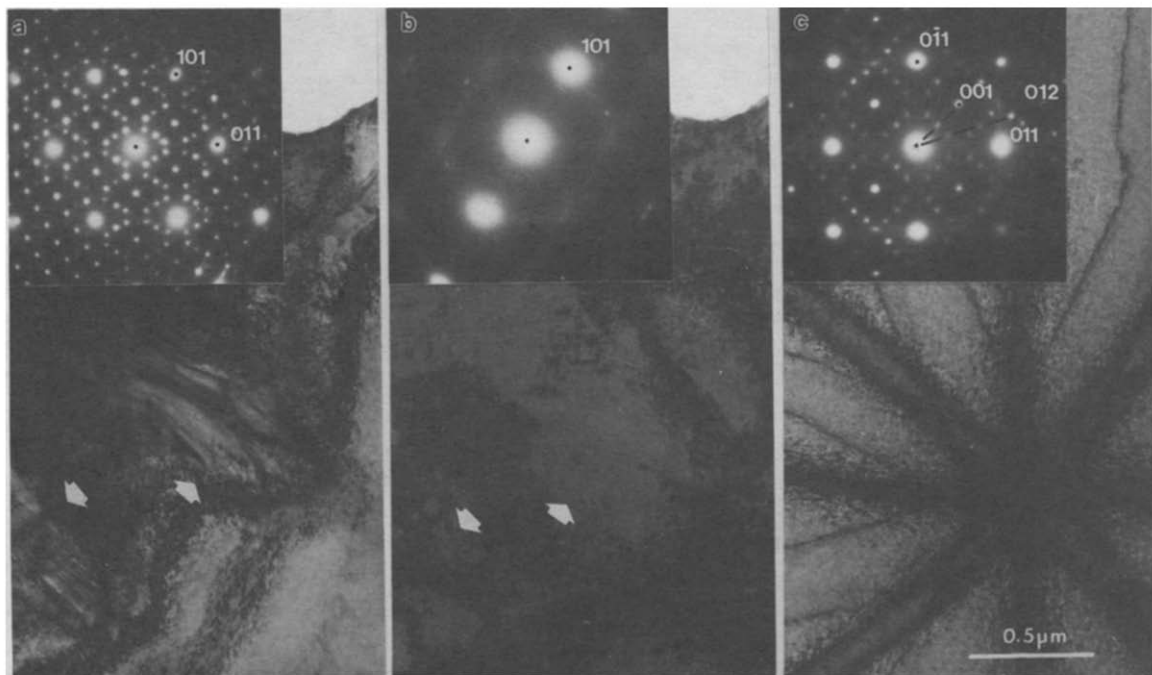


FIG. 7. TEM micrograph and SAD pattern of the new phase (a) before heat treatment, (b) after in situ heat treatment at 300 °C and (c) the same area after room temperature ageing for two weeks.